https://jksus.org

Journal of King Saud University – Science

2025 37 (1) 1402024

Original Article

Analytical approach to parabolic flows along with inclined plate with uniform diffusion of mass

Gunaseelan Mani[a], Sivakumar Pushparaj[b], Muthucumaraswamy Rajamanickam[c], Sabri T.M. Thabet[a,d,e,*], Miguel Vivas-Cortez[f,*]

[a]Department of Mathematics, Saveetha School of Engineering, Saveetha Institute of Medical and Technical Sciences, Saveetha University, Chennai, Tamil Nadu 602105, India
[b]Department of Mathematics, Panimalar Engineering College, Chennai, 600 123, Tamil Nadu, India
[c]Department of Applied Mathematics, Sri Venkateswara College of Engineering, Sriperumbudur, 602 117, Tamil Nadu, India
[d]Department of Mathematics, Radfan University College, University of Lahej, Lahej, Yemen
[e]Department of Mathematics, College of Science, Korea University, 145 Anam-ro, Seongbuk-gu, Seoul 02814, Republic of Korea
[f]Faculty of Exact and Natural Sciences, School of Physical Sciences and Mathematics, Pontifical Catholic University of Ecuador, Av. 12 de octubre 1076 y Roca, Apartado Postal 17-01-2184, Sede Quito, Ecuador

ARTICLE INFO

Keywords:
Heat and mass transfer
Inclined plate
Laplace transform
Matlab
Parabolic flows

ABSTRACT

This article investigates fluid flow over an infinite inclined plate with uniform mass diffusion, incorporating the effects of chemical reactions and parabolic motion while maintaining constant temperature and concentration at the plate. The flow is modeled through partial differential equations and framed with appropriate initial and boundary conditions. Using non-dimensional variables, the equations were transformed, and the Laplace transform method was employed to obtain solutions for the dimensionless heat, velocity, and concentration profiles. Analytical expressions for these profiles were derived using complementary error and exponential functions. Results were illustrated through MATLAB-generated graphs, enabling the analysis of velocity, temperature, and concentration profiles under varying parameters to explore their physical characteristics.

1. Introduction

Heat and mass flow often occur simultaneously in many engineering applications. An often-observed phenomenon is the process of lake water evaporating into the wind streaming across it. Water vapor diffuses into the air due to the partial pressure difference between the water's surface and atmosphere. As the surface water evaporates, it absorbs heat from the remaining water, lowering the temperature of the lake. This cooling effect leads to convection, through which air is heated and then transferred to the water. As the lake water temperature drops, the saturation partial pressure of the vapor at the water's surface also decreases, further slowing the mass transfer rate. Equilibrium is reached when heat flowing from the air to the liquid is sufficient for providing the latent heat required for evaporation, allowing liquid to disperse into the air.

Significant attention has been given to coupled mass and heat transfer issues due to their importance in various processes. Combined buoyancy mechanisms are involved in many applications, such as the curing of plastics and the production of bulb-insulated cables. For instance, if a colored substance like copper sulfate is placed at the bottom of a bottle filled with water and left undisturbed, the color will slowly spread from the bottom to the top, eventually resulting in uniformly colored water. This process, known as diffusion, describes the transfer of the colored substance from regions of higher concentration to regions of lower concentration. The flow phenomenon is characterized by various parameters, including velocity, concentration, and temperature distributions, Prandtl number, Schmidt number, time progression, and angle of inclination. Visual representations of the concentration, temperature, and velocity profiles have also been provided.

Impulsively started vertical plate flow, free convection currents, and the consequences of mass transfer were studied (Soundelgekar, 1979). Soundelgekar et al. (1979) further evaluated a mass transfer that started abruptly on a boundless perpendicular plate with varying temperatures. Das et al. (1994) impulsively started implications of mass transfer over a vertical infinite plate with a continuous mass flux in the flow. Xiao-Jun Yang (2017) analyzed a novel integral transform operator designed to address the heat-diffusion problem. This operator provides a new method for addressing heat-diffusion equations, contributing to more effective solutions in thermal analysis. Das et al. (1991) obtained an accurate solution for the dynamics of a viscous, incompressible fluid flowing past an impulsively initiated, infinitely thick vertical plate, considering uniform mass diffusion and a first-order chemical reaction. Meanwhile, scientists Xiao-Jun Yang et al. (2023) explored an odd entire-function solution to the one-dimensional diffusion equation within the context of the modular form theory. A numerical study by Muthucumaraswamy et al. (2016) investigated how flow through an abruptly commencing mass diffusion in a vertical plate might be affected by a first-order chemical reaction. Raptis et al. (1981) initiated the movement of a hydromagnetic convection past a vertical, accelerating plate with varying suction and flux. Mathematical methods were employed to solve the governing equations. Scientists also (Xiao-Jun Yang et al., 2023) examined special solutions for the Laplace

***Corresponding author:**
E-mail address: th.sabri@yahoo.com (Sabri T. M. Thabet); mjvivas@puce.edu.ec (Miguel Vivas-Cortez)

Received: 6 October, 2024 **Accepted:** 18 February, 2025 **Published:** 22 March, 2025

DOI: 10.25259/JKSUS_140_2024

and diffusion equations within the framework of algebraic number fields. The effects of continuous laminar free convection airflow with thermal radiation and chemical species concentration across an infinite vertical plate were studied (Chamkha et al., 2001). Sivakumar et al. (2014) examined radiative heat transfer's impacts across an endless isothermal vertical plate. Xiao-Jun Yang et al. (2023) gave solutions for the diffusion equation in relation to L-functions associated with cusp forms. A further analysis, (Muthucumaraswamy et al., 2016) studied magnetohydrodynamics flow through a parabolic and an unbound plate in the existence of heat radiation. Scientists (Rajput et al., 2016) investigated the unsteady MHD flow past an impulsively inclined plate, considering the effects of variable temperature, mass diffusion, and Hall currents. Thenmozhi et al. (2024) examined the MHD Darcy-Forchheimer flow of a micropolar fluid using a predictor-corrector finite difference method, incorporating the effects of viscous dissipation and heterogeneous-homogeneous reactions. Xiao-Jun Yang (2024) examined a new approach to entire functions in the field of number theory and a further analysis, explored new conjectures concerning entire functions linked to fractional calculus. Siva Sankari et al. (2023) and Thenmozhi et al. (2024) analyzed the double stratification of Casson nanofluid flow over an exponentially stretching sheet through analytical methods.

2. Formulation of the problem

The vertical axis is taken in an upward trajectory, and the y-axis is oriented perpendicular to the plate, while the x-axis runs along the plate at an angle of inclination. At time $t' \le 0$, both the fluid and the plate are at a uniform temperature. θ_∞. At time $t' > 0$, the plate is started with a velocity of $v = v_0.t'^2$ against the gravitational field in its own plane, and the ambient temperature of the plate is increased to θ_w and the concentration levels adjacent to the plate are also elevated. to C_w^*. Following Boussinesq's approximation, there are three equations that regulate the unstable motion: the momentum equation, the mass diffusion equation along with chemical reactions and the energy equation that includes radiation.

$$\frac{\partial v}{\partial t'} = g\beta\, Cos\alpha\left(\theta-\theta_\infty\right)+g\beta\, Cos\alpha\left(C^*-C_\infty^*\right)+\gamma\frac{\partial^2 v}{\partial y^2} \tag{1}$$

$$\rho C_p\ \frac{\partial\theta}{\partial t'} = k\,\frac{\partial^2\theta}{\partial y^2}. \tag{2}$$

$$\frac{\partial C^*}{\partial t'} = D\ \frac{\partial^2 C^*}{\partial y^2}. \tag{3}$$

These are the starting and limiting conditions:

$$v = 0\,,\theta = \theta_\infty, C^* = C_\infty^* \text{ for all } Y, t \le 0.$$

$$t' > 0 : v = v_0.t'^2\ ,\ \ \theta = \theta_w, C^* = C_w^*. \tag{4}$$

$$v \to 0, \theta \to \theta_\infty, C^* \to C_\infty^*\ \text{ as } y \to \infty.$$

To express equations (1), (2), and (3) in non-dimensional form, we will now introduce the non-dimensional variables.

These Non-dimensional form parameters are missing in Equation (5).

$$V = v\left(\frac{v_0}{\gamma^2}\right)^{\frac{1}{3}},\ t = \left(\frac{v_0^2}{\gamma}\right)^{\frac{1}{3}}t',\ Y = y\left(\frac{v_0}{\gamma^2}\right)^{\frac{1}{3}},\ \Pr = \frac{\mu C_p}{k},\ T = \frac{\theta-\theta_\infty}{\theta_w-\theta_\infty},$$

$$Gr = \frac{g\beta(\theta_w-\theta_\infty)}{(\gamma.v_0)^{1/3}},\ Gc = \frac{g\beta\left(C_w^*-C_\infty^*\right)}{(\gamma.v_0)^{1/3}},\ Sc = \frac{\gamma}{D}. \tag{5}$$

When we insert equation (5) into equations (1), (2), and (3), the governing equations take on a non-dimensional form.

$$\frac{\partial V}{\partial t} = GrT\ Cos\ \alpha + Gc\varphi\ Cos\ \alpha + \frac{\partial^2 V}{\partial Y^2}. \tag{6}$$

$$\Pr\frac{\partial T}{\partial t} = \frac{\partial^2 T}{\partial Y^2}. \tag{7}$$

$$Sc\frac{\partial\varphi}{\partial t} = \frac{\partial^2\varphi}{\partial Y^2}. \tag{8}$$

The preliminary and boundary circumstances based on equation (4), it is now expressed as

$$V = 0, T = 0, \varphi = 0 \text{ for every } Y, t \le 0.$$

$$t > 0 :\quad V = t^2, T = 1, \varphi = 1 \text{ at } Y = 0. \tag{9}$$

$$V \to 0,\ \ T \to 0, \varphi \to 0 \text{ as } \ Y \to \infty.$$

3. Solution of the problem

The dimensionless fundamental equations (6) to (8), along with the equation (9), are solved. The resulting solution is presented below.

$$T = L_2$$

$$\varphi = L_3$$

$$V = 2\left(\frac{t^2}{6}\left[L_1\left(L_{05}\right)-L_4(L_{00})\left(L_{04}\right)\right]\right)-(a+b)\left[t\left[L_1\left(L_{01}\right)-2L_4(L_{00})\right]\right]$$
$$+a\left(t\left[L_2\left(L_{02}\right)-2L_5(L_{00})\sqrt{\Pr}\right]\right)+b\left(t\left[L_3\left(L_{03}\right)-2L_6(L_{00})\sqrt{Sc}\right]\right)$$

Where, $a = -\frac{Gr\ Cos\,\alpha}{(\Pr-1)}$, $b = -\frac{Gc\ Cos\alpha}{(Sc-1)}$ and $\eta = \frac{Y}{2\sqrt{t}}$.

4. Results and analysis of the problem

Fig. 1 shows the physical model and the coordinate system used to describe the problem. Fig. 2(a) and 2(b) velocity profiles are plotted respectively. It is very esvident that when Pr falls in the boundary layer and raises the velocity profile. In Fig. 3(a) and 3(b) represents the impact of velocity with respect to time. Increases in speed are consistently measured throughout time. The velocity curves for various plate angles are represented in Fig. 4(a) and 4(b). It has been seen that when the plate angle is raised, the velocity decreases. Fig. 5(a) and 5(b) velocity profiles are plotted respectively. It is very evident that when Sc falls in the boundary layer and raises the velocity profile.

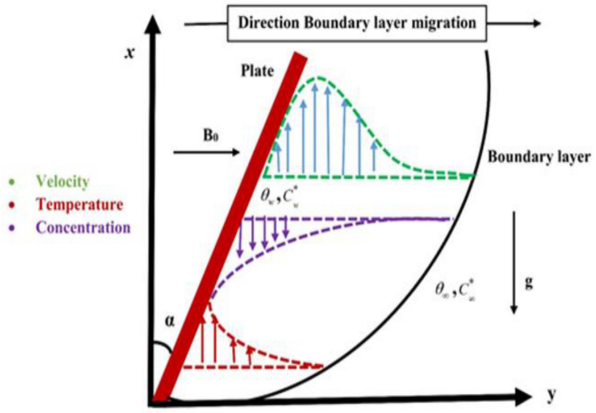

Fig. 1. Governing system and physical model.

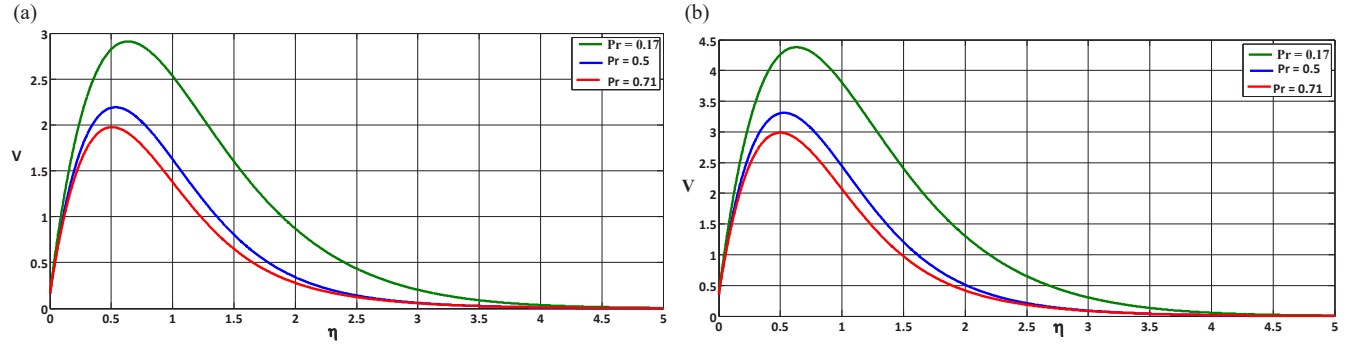

Fig. 2. (a) Shows a comparison of velocity for different *Pr* values at t = 0.4, (b) Shows a comparison of velocity for different *Pr* values at t = 0.6.

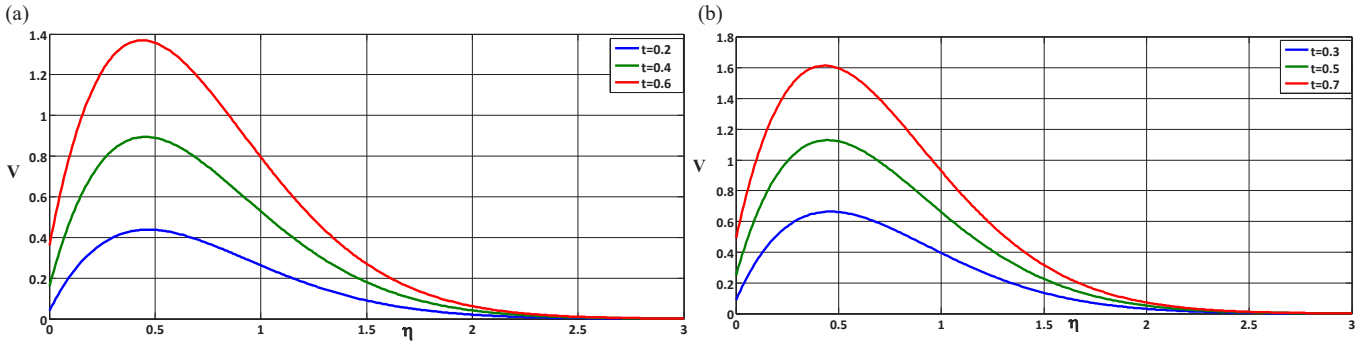

Fig. 3. (a) Shows a comparison of velocity for different *t* values, (b) Shows a comparison of velocity for different *t* values.

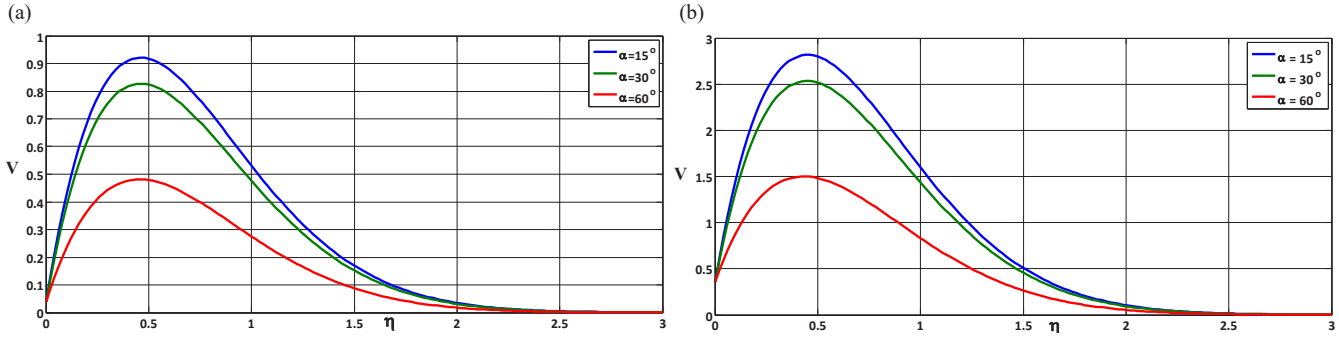

Fig. 4. (a) Presents a comparison of velocity for various α values, (b) Shows a comparison of velocity for different α values.

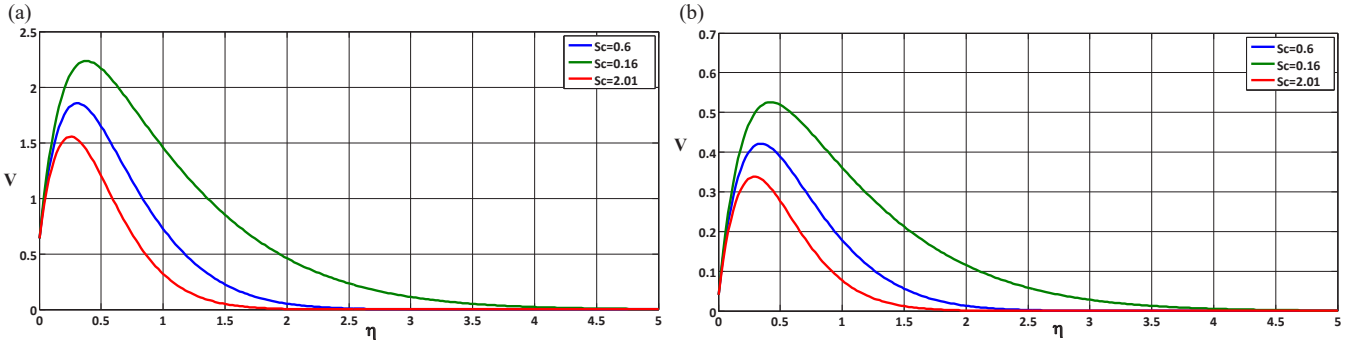

Fig. 5. (a) Shows a comparison of velocity for different Sc values at t = 0.6, (b) Shows a comparison of velocity for different *Sc* values at t = 0.2.

Figs. 6(a), 6(b), 7(a), and 7(b) present several values of the Gr and Gc. This is clear that the velocity magnifies when the Gr or Gc increases because of buoyancy force. Fig. 8(a) and 8(b) displays the result of Sc on the concentration profiles respectively. It is investigational that the concentration curves diminish as the (Sc) increases. The fluid's temperature for Pr is proffered at Fig. 9(a) and 9(b), this is clearly demonstrating that temperature profile decreased as increase Pr.

Table 1 presents Pr's velocity changes over time, with data shown in Fig. 2(a) and 2(b). Table 2 shows the velocity of t for different time values, linked to Fig. 3(a) and 3(b). Table 3 provides a comparison

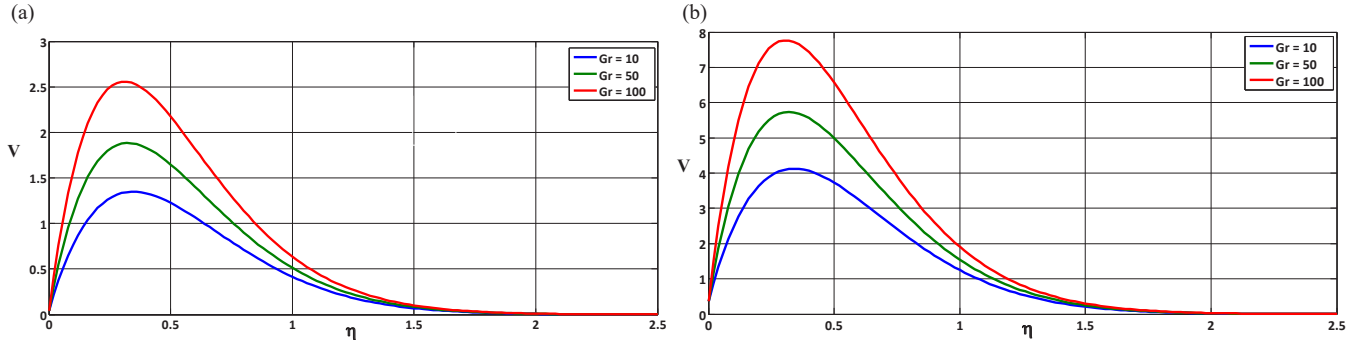

Fig. 6. (a) Displays a comparison of velocity for different *Gr* values at t = 0.2, (b) Shows a comparison of velocity for different *Gr* values at t = 0.6.

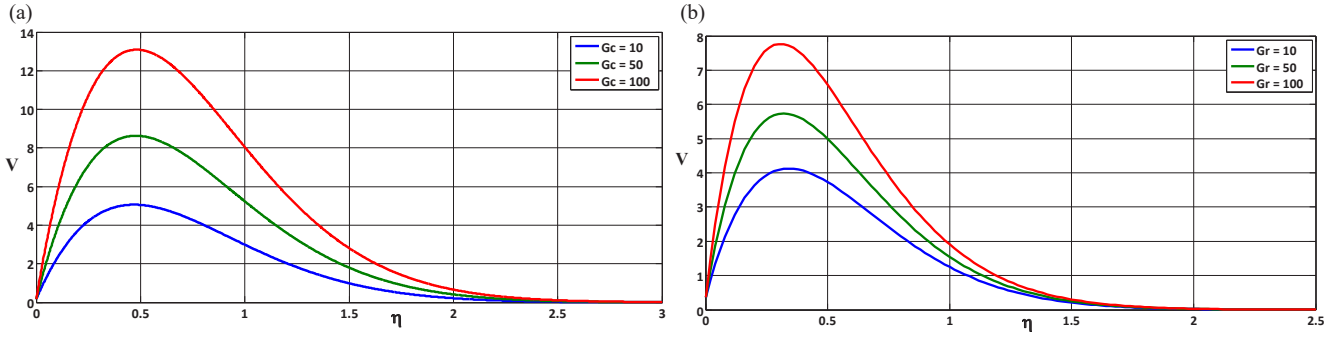

Fig. 7. (a) Shows a comparison of velocity for different *Gc* values at t = 0.4, (b) Shows a comparison of velocity for different *Gc* values at t = 0.6.

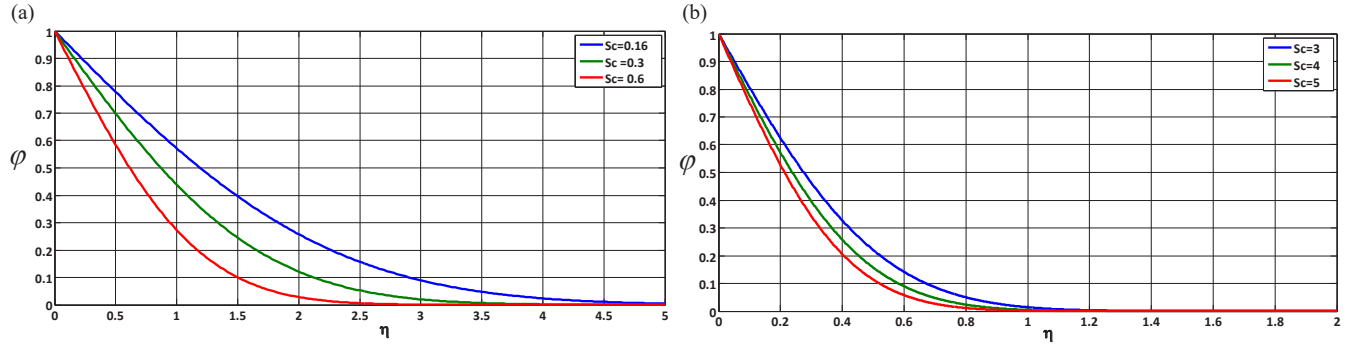

Fig. 8. (a) Shows a comparison of concentration for different *Sc* values, (b) Shows a comparison of concentration for different *Sc* values.

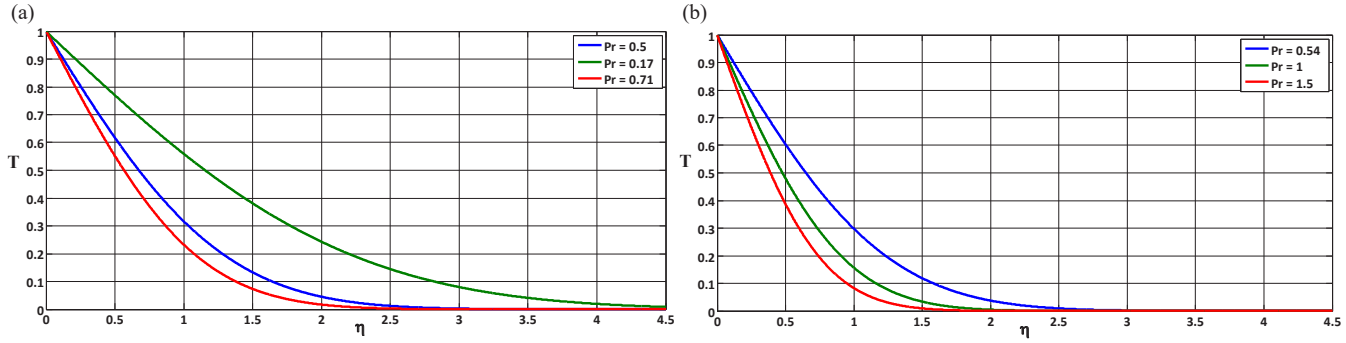

Fig. 9. (a) Shows a comparison of temperature for different *Pr* values, (b) Shows a comparison of temperature for different *Pr* values.

Table 1.
Displays numerical values comparison of Pr's velocity for different time values

Non-dimensional parameter	Fig. 2(a)	Fig. 2(b)
Pr	0.5, 0.17, 0.71	0.5, 0.17, 0.71
Gc	5	5
Gr	15	15
Sc	0.16	0.16
t	**0.4**	**0.6**
α	30^0	30^0
Conclusion	Velocity reduces as the flow of the Prandtl numbers rises	

Table 2.
Displays numerical values comparison of t's velocity for different time values.

Non dimensional parameter	Fig. 3(a)	Fig. 3(b)
t	**0.2, 0.4, 0.6**	**0.3, 0.5, 0.7**
Pr	0.71	0.71
Gc	5	5
Gr	5	5
Sc	0.6	0.6
α	30^0	30^0
Conclusion	Velocity increases along with the flow of time.	

Table 3.
Displays numerical values comparison between α's velocity for different time values.

Non dimensional parameter	Fig. 4(a)	Fig. 4(b)
α	15^0, 30^0, 60^0	15^0, 30^0, 60^0
Pr	0.71	0.71
Gc	5	5
Gr	15	15
Sc	0.78	0.78
t	**0.2**	**0.6**
Conclusion	The velocity drops as the plate angle improves.	

of α's velocity over time, supported by Fig. 4(a) and 4(b). Table 4 displays how Sc's velocity varies, with Fig. 5(a) and 5(b) illustrating the results. Tables 5 and 6 compare the velocities of Gr and Gc over time, using Figs. 6(a), 6(b), 7(a), and 7(b) for reference. Table 7 focuses on concentration variations due to Sc, supported by Fig. 8(a) and 8(b). Lastly, Table 8 highlights temperature changes based on different Pr values, shown in Fig. 9(a) and 9(b).

Table 4.
Displays numerical values comparison of Sc's velocity for different time values.

Non dimensional parameter	Fig. 5(a)	Fig. 5(b)
Sc	0.6, 0.16 2.01	0.6, 0.16 2.01
Pr	5	5
Gc	5	5
Gr	15	15
t	**0.6**	**0.2**
α	30^0	30^0
Conclusion	As the flow of Schmidt numbers increases, velocity decreases.	

Table 5.
Displays numerical values comparison of Gr's velocity for different time values.

Non dimensional parameter	Fig. 6(a)	Fig. 6(b)
Gr	10, 50, 100	10, 50, 100
Pr	5	5
Gc	50	50
Sc	2.01	2.01
t	**0.2**	**0.6**
α	30^0	30^0
Conclusion	It is evident that as Gr rises, the velocity improves.	

Table 6.
Displays numerical values comparison of Gc's velocity for different time values.

Non dimensional parameter	Fig. 7(a)	Fig. 7(b)
Gc	10, 50, 100	10, 50, 100
Pr	0.71	0.71
Gr	50	50
Sc	0.6	0.6
t	**0.4**	**0.6**
α	30^0	30^0
Conclusion	It is apparent that the velocity rises as Gc increases.	

Table 7.
Displays numerical values comparison of concentration for different Sc's values.

Non dimensional parameter	Fig. 8(a)	Fig. 8(b)
Sc	0.16, 0.3, 0.6	3, 4, 5
Conclusion	The finding that concentration ratios are thinner as the Schmidt number (Sc) increases is exploratory.	

Table 8.
Displays numerical values comparison of temperature for different Pr's values.

Non dimensional parameter	Fig. 9(a)	Fig. 9(b)
Pr	0.5, 0.17, 0.71	0.54, 1, 1.5
Conclusion	This proves unequivocally that the temperature profile fell as the Pr increased.	

5. Conclusion

The intention of the complete review in closed form is to investigate the effect of an inclined plate with uniform mass diffusion, and the solutions are obtained through the Laplace procedure. The consequences of the problem are presented below.

- The velocity improves as well as a rise in (Gr), (Gc), and time (t). It exhibits the opposite effect when (Pr) and (Sc) increases.
- Temperature profile diminishes with an increase of (Pr).
- As the (Sc) increases, the concentration profile diminishes.

5.1 Future works

- The combined analysis of chemical processes and thermal radiation effects, along with heat and mass transfer, has significant applications in aerospace and space research, particularly because space vehicles follow parabolic paths to achieve orbit.
- The role of mass diffusion becomes particularly important in the occurrence of chemical reactions.
- This study examines different chemically reactive species and their impact on the concentration field, which has practical implications for the chemical processing industry.

CRediT authorship contribution statement

Gunaseelan Mani: Formal analysis, reviewing & editing, Validation. **Sivakumar Pushparaj:** Conceptualization, Investigation, writing original draft, reviewing & editing, Validation, Software, Methodology, Supervision. **Muthucumaraswamy Rajamanickam:** Formal analysis, reviewing & editing, Validation. **Sabri T.M. Thabet:** Formal analysis, reviewing & editing, Validation. **Miguel Vivas-Cortez:** Formal analysis, reviewing & editing, Validation.

Declaration of competing interest

The authors declare that they have no known competing financial interests or personal relationships that could have appeared to influence the work reported in this paper.

Declaration of Generative AI and AI-assisted technologies in the writing process

The authors confirm that there was no use of artificial intelligence (AI)-assisted technology for assisting in the writing or editing of the manuscript and no images were manipulated using AI.

Funding

"La derivada fraccional generalizada, nuevos resultados y aplicaciones a desigualdades integrales" Cod UIO-077-2024.

Supplementary material

Supplementary available on: https://doi.org/10.25259/JKSUS_140_2024

References

Chamkha, A.J., Takhar, H.S., Soundalgekar, V.M., 2001. Radiation effects on free convection flow past a semi-infinite vertical plate with mass transfer. Chem. Eng. J. 84, 335-342. https://doi.org/10.1016/s1385-8947(00)00378-8

Das, U.N., Deka, R., Soundalgekar, V.M., 1994. Effects of mass transfer on flow past an impulsively started infinite vertical plate with constant heat flux and chemical reaction. Forsch Ing-Wes 60, 284-287. https://doi.org/10.1007/bf02601318

Das, U.N., Ray, S.N., Soundalgekar, V.M., 1991. MHD Flow past and impulsively started vertical plate in the presence of mass transfer and viscous dissipation. Proc. Math. Soc., Banarus Hindu University (BHU). 7, 71-75.

Muthucumaraswamy, R., Ganesan, P., 2001. First-order chemical reaction on flow past an impulsively started vertical plate with uniform heat and mass flux. Acta Mechanica 147, 45-57. https://doi.org/10.1007/bf01182351

Muthucumaraswamy, R., Sivakumar, P., 2016. MHD flow past a parabolic flow past an infinite isothermal vertical plate in the presence of thermal radiation and chemical reaction. Int. J. Appl. Mech. Eng. 21, 95-105. https://doi.org/10.1515/ijame-2016-0006

Muthucumaraswamy, R., Sivakumar, P., 2014. Radiative heat transfer effects on a parabolic flow past an infinite isothermal vertical plate in the presence of chemical reaction. IJESRT, 2014, 3, 1354-1358.

Rajput, U.S., Gaurav, K., 2016. Unsteady MHD flow past an impulsively inclined plate with variable temperature and mass diffusion in the presence of hall current". Appl. Appl. Math. 11, 693-703.

Raptis, A.A., Tzivanidis, G.J., Perdikis, C.P., 1981. Hydromagnetic free convection flow past an accelerated vertical infinite plate with variable suction and heat flux. Lett. Heat Mass Transf. 8, 137-143. https://doi.org/10.1016/0094-4548(81)90035-7

Siva Sankari, M., Rao, M.E., Khan, W., Alshehri, M.H., Eldin, S.M., Iqbal, S., 2023. Analytical analysis of the double stratification on casson nanofluid over an exponential stretching sheet. Case Stud. Therm. Eng. 50, 103492. https://doi.org/10.1016/j.csite.2023.103492

Soundalgekar, V.M., Ali, M.A., 1990. Free convection effects on MHD flow past an impulsively started infinite vertical plate with constant heat flux. Model. Simul. and Cont.. 37, 53-64.

Soundalgekar, V.M., 1979. Effects of mass transfer and free-convection currents on the flow past an impulsively started vertical plate. Trans. ASME J. Applied Mechanics 46, 757-760. https://doi.org/10.1115/1.3424649

Thenmozhi, D., Eswara Rao, M., 2024. Predictor-corrector FDM analysis of MHD darcy-forchheimer flow of a micropolar fluid with viscous dissipation and heterogeneous-homogeneous. Propuls. Power Res. 13, 257-272. https://doi.org/10.1016/j.jppr.2023.12.002

D, T., Eswara Rao, M., Nagalakshmi, C., Devi, R.L.V.R., Selvi, P.D., 2024. Lie similarity analysis of MHD casson fluid flow with heat source and variable viscosity over a porous stretching sheet. International Journal of Thermofluids 23, 100804. https://doi.org/10.1016/j.ijft.2024.100804

Yang, X.-J., 2017. A new integral transform operator for solving the heat-diffusion problem. Appl. Math. Lett. 64, 193-197. https://doi.org/10.1016/j.aml.2016.09.011

Xiao-Jun Yang., 2024. A new program for the entire functions in number theory, Fractals, 32, 2340122-1-2340122-12.

Yang, X.-J., Sweilam, N., Bayram, M., 2023. Special solutions for the laplace and diffusion equations associated with the algebraic number field. Therm Sci. 27, 477-481. https://doi.org/10.2298/tsci221113006y

Yang, X.-J., Abdel-Aty, M., Hayat, T., 2023. On the solution for the diffusion equation related to the l-functions attached to cusp forms. Therm. Sci. 27, 521-526. https://doi.org/10.2298/tsci221106012y

Yang, X.-J., Hayat, T., 2023. An odd entire-function solution for one-dimensional diffusion equation in theory of modular form. Therm. Sci. 27, 465-468. https://doi.org/10.2298/tsci221105004y

Xiao-Jun Yang., 2024 New conjectures for the entire functions associated with fractional calculus. Fractals 32, 2340129-1-2340129-7.